A&A 414, 667–676 (2004)
DOI: 10.1051/0004-6361:20031654


Astronomy & Astrophysics

# X-ray observations of Be/X-ray binaries in the SMC⋆

F. Haberl and W. Pietsch

Max-Planck-Institut für extraterrestrische Physik, Giessenbachstraße, 85748 Garching, Germany

Received 14 July 2003 / Accepted 21 October 2003

**Abstract.** Fifteen Be/X-ray binaries and candidates in the SMC were observed serendipitously with the EPIC instruments of XMM-Newton during two observations of SNR 0047−73.5 and SNR 0103–72.6 in October 2000. A total of twelve of those sources are detected. For eleven of them an accurate position and in part detection of X-ray pulsations support the proposed identification as Be/X-ray binaries. In one case the improved X-ray position excludes the previously suggested identification with an H$\alpha$ emission line star found within the ROSAT error circle. The detection of pulsations (172.2 s, 320.1 s and 751 s) from three hard X-ray sources with periods known from ASCA observations confirm their proposed identifications with ROSAT sources and their optical Be star counterparts. In addition, pulsations with a period of 263.6 s were found from XMMU J004723.7−731226 = RX J0047.3−7312. For SAX J0103.2−7209 a pulse period of $341.2 \pm 0.5$ s was determined, continuing the large spin-up seen with ASCA, BeppoSAX and Chandra between 1996 and 1999 with a period derivative of $-1.6$ s yr$^{-1}$ covering now 4.5 years. The 0.3–10.0 keV EPIC spectra of all eleven Be/X-ray binaries and candidates are consistent with power-law energy distributions with derived photon indices strongly peaked at 1.00 with a standard deviation of 0.16. No pulsations are detected from RX J0049.2−7311 and RX J0049.5−7310 (both near the 9 s pulsar AX J0049−732) and RX J0105.1−7211 (near AX J0105−722, which may pulsate with 3.3 s), leaving the identification of the ASCA sources with ROSAT and corresponding XMM-Newton objects still unclear. We present an updated list of high-mass X-ray binaries (HMXBs) and candidates in the SMC incorporating improved X-ray positions obtained from Chandra and XMM-Newton observations. Including the results from this work and recent publications the SMC HMXB catalogue comprises 65 objects with at least 37 showing X-ray pulsations.

**Key words.** galaxies: individual: Small Magellanic Cloud – stars: neutron – X-rays: binaries – X-rays: galaxies

## 1. Introduction

X-ray observations of the Small Magellanic Cloud (SMC) with recent observatories like ASCA, BeppoSAX, ROSAT and RXTE revealed a large number of Be/X-ray binary systems. Most of them were discovered through the detection of X-ray pulsations (e.g. see summary of ASCA X-ray sources in the SMC, Yokogawa et al. 2003), indicating the spin period of the neutron star which orbits an early type star. Optical follow-up observations are then required to determine the spectral type of the high-mass star. In the SMC only Be stars were identified (with the only secure exception of the supergiant system SMC X-1), making the SMC very different to the Milky Way and the Large Magellanic Cloud in absolute numbers of high mass X-ray binaries with respect to the galaxy mass and also in their ratio of Be to supergiant OB systems.

Haberl & Sasaki (2000, hereafter HS00) searched for Be/X-ray binaries in the ROSAT catalogues of Haberl et al. (2000) and Sasaki et al. (2000) by correlating them with catalogues of optical H$\alpha$ emission-line objects (Meyssonnier & Azzopardi 1993; Murphy & Bessell 2000). HS00 presented a list of 47 Be/X-ray binaries and candidates with X-ray positions typically better than 10″. Since the launch of Chandra and XMM-Newton new X-ray pulsars and Be/X-ray binary candidates were discovered (Sasaki et al. 2001, 2003; Macomb et al. 2003). Together with eleven pulsars detected by RXTE with very uncertain X-ray positions we know about sixty high mass X-ray binaries (HMXBs) and candidates in the SMC, from which more than thirty are known as X-ray pulsars (Yokogawa et al. 2003; Mereghetti 2001).

The position uncertainties of X-ray sources in the SMC obtained by previous missions of up to tens of arcseconds (including the most precise ROSAT positions) made it in many cases impossible to uniquely correlate sources from the different X-ray missions, nor allowed exact optical identifications. We therefore started to systematically analyze archival XMM-Newton data of HMXBs and candidates in the SMC in order to confirm their proposed nature. First results were presented in Sasaki et al. (2003). Here we continue this work analyzing the XMM-Newton EPIC data of two fields in the SMC which contain in total fifteen known HMXBs and candidates.

*Send offprint requests to*: F. Haberl, e-mail: fwh@mpe.mpg.de

⋆ Based on observations with XMM-Newton, an ESA Science Mission with instruments and contributions directly funded by ESA Member states and the USA (NASA).

## 2. XMM-Newton observations and analysis

XMM-Newton observed the fields around the SMC supernova remnants SNR 0047−73.5 and SNR 0103−72.6 on October 15,

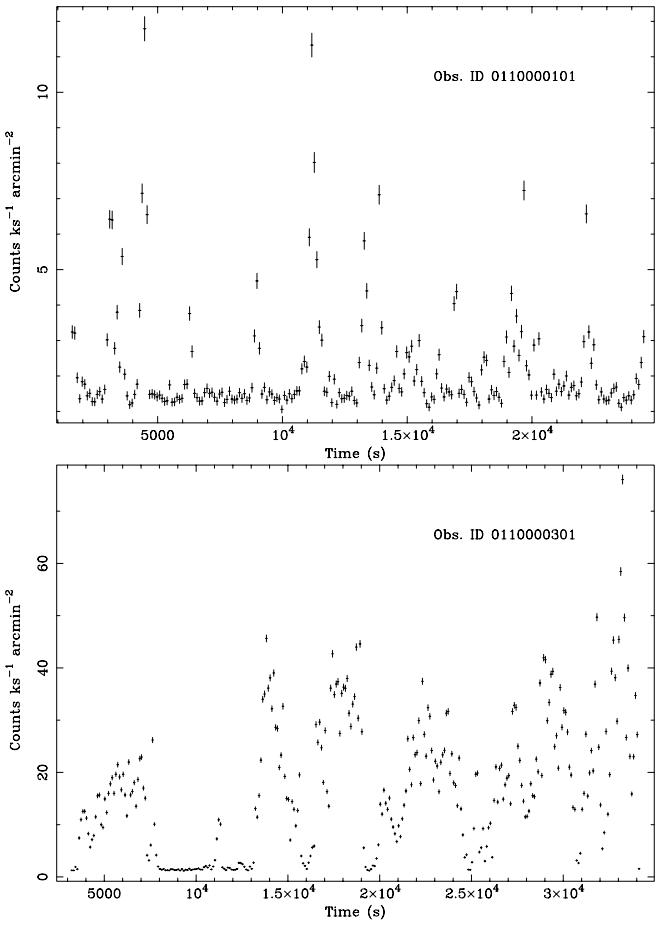


**Fig. 1.** EPIC-pn background light curves obtained from source free regions in the 7.0–15.0 keV band for the two investigated observations of SNR 0047−73.5 (0110000101) and SNR 0103−72.6 (0110000301).

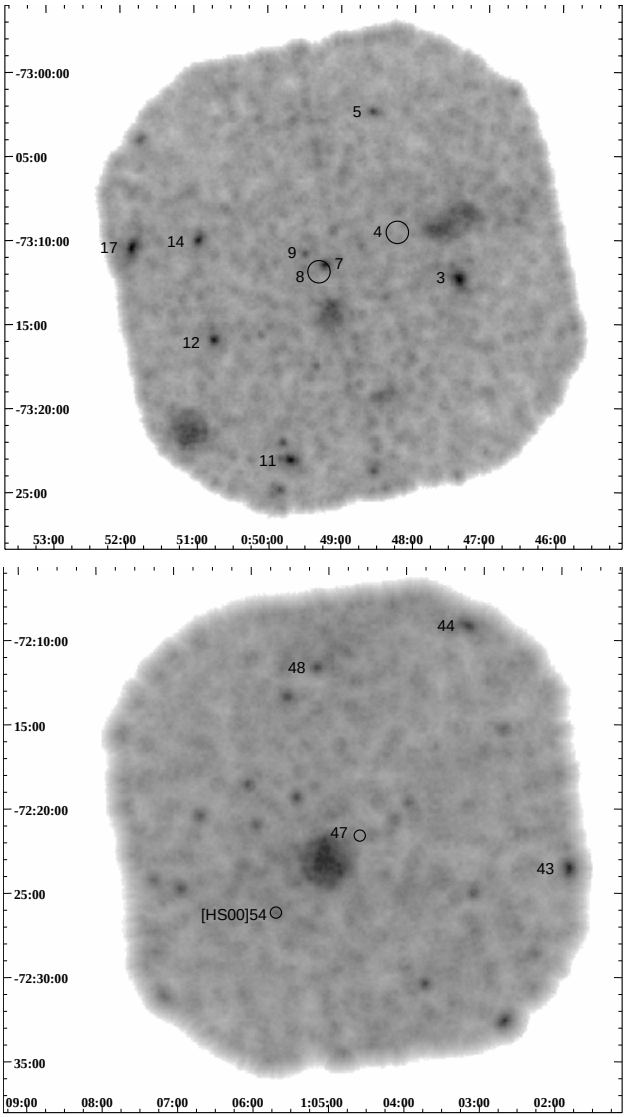


**Fig. 2.** EPIC-pn images of the two observed SMC fields obtained from 1.0–2.0 keV data, using an intensity dependent adaptive smoothing (top: observation 0110000101 with SNR 0047−73.5 near the center of the image; bottom: observation 0110000301 with SNR 0103−72.6). The Be/X-ray binaries and candidates are marked with numbers as used in Table 3. Source 54 from HS00 was removed as Be/X-ray binary candidate from Table 3 because its improved position derived from the EPIC data is now inconsistent with that of the emission line object proposed as optical counterpart. Sources 4, 8 and 47 were not detected, while a possible association of source 8 (detected with ASCA) with source 7 or 9 (ROSAT) could not be clarified (see Sect. 2.1).

2000 and on October 17, 2000 with EPIC-MOS (MOS1 and MOS2, Turner et al. 2001) for 26.9 ks and 34.8 ks and EPIC-pn (Strüder et al. 2001) for 23.0 ks and 30.9 ks. For both observations the three EPIC cameras were operated in imaging mode covering the full field of view of ∼14′ radius, MOS in full-frame (2.6 s time resolution) and pn in extended full-frame (0.2 s) CCD readout mode. For optical light blocking the medium filter was used in all cameras.

The data were processed using the XMM-Newton analysis package SAS version 5.4.1 to produce the photon event files and binned data products like images, spectra and light curves. To avoid artificial photon arrival time jumps in the EPIC pn data an updated SAS development version from 2003, May 16 was used to create pn event files.

The observation of SNR 0103−72.6 suffered from strong background flaring activity (Fig. 1) which hampered the analysis of the data. We applied two different levels of background screening depending on the goals of the analysis. To obtain clean images which also show faint sources we used only data from times of low background (<10 cts ks$^{-1}$ arcmin$^{-2}$ in EPIC-pn). To search for periodicities in the brighter sources we used two different background cuts of 10 and 50 cts ks$^{-1}$ arcmin$^{-2}$. While the strong screening removes the flares which have typical time scales of a few 1000 s, the latter method avoids too many data gaps. For the spectral analysis of point sources the cut level of 50 cts ks$^{-1}$ arcmin$^{-2}$ was applied. For the MOS data corresponding levels of 2 and 5 cts ks$^{-1}$ arcmin$^{-2}$ were defined, which result in similar good time intervals in the contemporaneous parts of MOS and pn data.

Figure 2 shows the EPIC-pn images of the two observed SMC fields. The investigated Be/X-ray binaries are marked with source numbers given in Table 3 which we use throughout the paper. The fields of view of the MOS cameras are

**Table 1.** Be/X-ray binaries and candidates detected in the EPIC fields.

| Column 1 | 2 | 3 | 4 | 5 | 6 | 7 | 8 | 9 | 10 |
|---|---|---|---|---|---|---|---|---|---|
| XMMU J... | RA (J2000.0) | Dec | Pos. err. [″] | Count rate [$s^{-1}$] | HS | MA | $d_{MA}$ [″] | Period [s] | Source Tab. 3 |
| 004723.7−731226 | 00 47 23.70 | −73 12 26.9 | 4.0 | $4.14\times10^{-1}\pm6\times10^{-3}$ | 6 | 172 | 3.9 | 263.64 ± 0.30 | 3 |
| 004834.5−730230[a] | 00 48 34.50 | −73 02 30.0 | 4.1 | $5.49\times10^{-2}\pm5\times10^{-3}$ | 8 | 238 | 2.2 | | 5 |
| 004913.8−731136 | 00 49 13.84 | −73 11 36.7 | 4.0 | $3.74\times10^{-2}\pm2\times10^{-3}$ | – | – | – | | 7 |
| 004929.9−731058 | 00 49 29.92 | −73 10 58.0 | 4.1 | $8.37\times10^{-3}\pm8\times10^{-4}$ | 10 | 300 | 1.7 | | 9 |
| 004942.3−732313 | 00 49 42.37 | −73 23 13.2 | 4.0 | $1.85\times10^{-1}\pm5\times10^{-3}$ | 12 | 315 | 2.6 | 750.9 ± 2.4 | 11 |
| 005045.2−731602 | 00 50 45.20 | −73 16 02.9 | 4.0 | $9.52\times10^{-2}\pm3\times10^{-3}$ | 13 | 387 | 3.0 | 320.12 ± 0.40 | 12 |
| 005057.6−731007 | 00 50 57.60 | −73 10 07.9 | 4.0 | $8.40\times10^{-2}\pm3\times10^{-3}$ | 15 | 414 | 1.7 | | 14 |
| 005152.2−731033 | 00 51 52.29 | −73 10 33.4 | 4.0 | $3.41\times10^{-1}\pm7\times10^{-3}$ | 19 | 504 | 2.1 | 172.21 ± 0.13 | 17 |
| 010152.4−722335 | 01 01 52.41 | −72 23 35.7 | 4.1 | $1.19\times10^{-1}\pm7\times10^{-3}$ | 45 | 1288 | 2.8 | | 43 |
| 010314.2−720914 | 01 03 14.21 | −72 09 14.5 | 4.1 | $8.44\times10^{-2}\pm7\times10^{-3}$ | 49 | 1367 | 1.1 | 341.21 ± 0.50 | 44 |
| 010509.7−721146 | 01 05 09.76 | −72 11 46.4 | 4.2 | $2.06\times10^{-2}\pm3\times10^{-3}$ | 53 | (1517) | 10.7 | | 48 |
| 010541.5−722617 | 01 05 41.56 | −72 26 17.3 | 4.2 | $3.52\times10^{-3}\pm5\times10^{-4}$ | 54 | (1544) | 14.3 | | – |

[a] Position and count rate from combined MOS data.

Notes to specific columns: (5) 0.3–7.5 keV count rates with $1\sigma$ errors. (6) Entry numbers from the compilation of Be/X-ray binaries from Haberl & Sasaki (2000). (7) Entry numbers from the H$\alpha$ emission line object catalogue of Meyssonnier & Azzopardi (1993). (8) Angular distance between X-ray and the optical position of the nearest emission line object. (9) Pulse period determined in this work.

slightly shifted with respect to pn and do not cover the 345 s pulsar SAX J0103.2−7209 (source 44).

### 2.1. Source positions

Source detection based on sliding window and maximum likelihood methods available in the SAS package was applied to the MOS and pn images, simultaneously for four energy bands (0.3–1.0 keV, 1.0–2.0 keV, 2.0–4.5 keV and 4.5–7.5 keV), but separately for the three instruments. Dividing the data into several energy bands enhances the signal-to-noise ratio for sources which have their major part of emission in a relatively narrow band, like e.g. super-soft X-ray sources or highly absorbed sources. In Table 1 we list the detected Be/X-ray binaries with XMM-Newton names, X-ray positions, count rates as obtained from the pn images (except for source 5 which is located near a CCD border in the pn camera). Coordinate uncertainties include a 4″ systematic error (Barcons et al. 2002). We correlated our source list with the compilation of Be/X-ray binaries from HS00 and with the H$\alpha$ emission line object catalogue of Meyssonnier & Azzopardi (1993). Source 47 (Fig. 2) detected in ROSAT HRI data (Sasaki et al. 2000) was not detected by the EPIC instruments. Source 4 (Yokogawa et al. 2003) was not detected either the association of the 9.1 s pulsar AX J0049−732 (source 8) with either source 7 or 9 (Yokogawa et al. 2003; Filipović et al. 2000b) could not be confirmed by a detection of the pulsations from either of the two sources in the EPIC data (see below). AX J0049−732 may be an uncorrelated source detected during a brighter state during the ASCA observations. HS00 classified RX J0105.7−7226 ([HS00]54) as candidate Be/X-ray binary due to the positional coincidence with the emission-line object 1544 in Meyssonnier & Azzopardi (1993). Our newly derived X-ray position fully agrees with the ROSAT position, but the smaller uncertainty now excludes an association with the emission-line object. Since no other evidence argues for RX 0105.7−7226 as Be/X-ray binary, we remove it from the list of candidates. Similarly, source 48 is now very unlikely to be associated with [MA93]1517. This makes the situation concerning the identification of the possible pulsar AX J0105−722 with a ROSAT source more unclear. However, the spectral analysis of RX J0105.1−7211 (see below) supports the HMXB nature of the source and we therefore keep it as a candidate.

There remain eleven Be/X-ray binaries and candidates in the two SMC fields for which we present a more detailed temporal and spectral analysis in the following.

### 2.2. X-ray pulsations

We searched for pulsations in the X-ray light curves (from different energy bands and background screening levels) of all eleven Be/X-ray binaries and candidates using Fast Fourier Transform (FFT) and Rayleigh $Z_n^2$ methods. The power spectra obtained from broad-band data (0.3–7.5 keV) of the three known pulsars in the field of SNR 0047−73.5 (sources 11, 12 and 17) clearly reveal their pulse periods. This – together with the accurate source positions – now allows the unique identification of the ASCA sources (which showed pulsations) with ROSAT sources (good X-ray positions), which could previously be done on positional coincidence only. In particular RX J0051.9−7311 (source 17), which was suggested to be the counterpart of the 16.6 s pulsar XTE J0050−732#1 (Lamb et al. 2002b) or the 172 s pulsar AX J0051.6−7311 (Yokogawa et al. 2003), is consistent in position with XMMU J005152.2−731033, which shows 172.2 s pulsations. In addition we find 263 s pulsations from XMMU J004723.7−731226 = RX J0047.3−7312 which is likely associated with AX J0047.3−7312 (see also

**Table 2.** Spectral fit results using an absorbed power-law model.

| Source Tab. 3 | $\gamma$ | $N_H$[c] [$10^{21}$ cm$^{-2}$] | $F_x$[d] [erg cm$^{-2}$ s$^{-1}$] | $L_x$[e] [erg s$^{-1}$] | $L_{x,ASCA}$[e] [erg s$^{-1}$] | $L_{x,ROSAT}$[e] [erg s$^{-1}$] | $L_x^{max}/L_x^{min}$ |
|---|---|---|---|---|---|---|---|
| 3 | $0.76 \pm 0.04$ | $2.2 \pm 0.3$ | $3.3 \times 10^{-12}$ | $1.8 \times 10^{36}$ | $3.4\text{-}6.8 \times 10^{35}$ | $1.5\text{-}12 \times 10^{35}$ | 12.0 |
| 5 | $0.89 \pm 0.19$ | <1.7 | $2.1 \times 10^{-13}$ | $1.0 \times 10^{35}$ | | $3.0 \times 10^{35}$ | 3.0 |
| 7 | $1.33 \pm 0.15$ | $7.7 \pm 1.7$ | $2.7 \times 10^{-13}$ | $1.8 \times 10^{35}$ | | $1.6\text{-}2.0 \times 10^{35}$ | 1.3 |
| 9[a] | $1.05^{+0.55}_{-0.43}$ | $5.4^{+6.3}_{-3.5}$ | $9.4 \times 10^{-14}$ | $5.6 \times 10^{34}$ | | $2.7\text{-}2.8 \times 10^{35}$ | 4.8 |
| 11 | $0.89 \pm 0.08$ | $3.6 \pm 0.6$ | $1.6 \times 10^{-12}$ | $9.0 \times 10^{35}$ | $6.8\text{-}7.7 \times 10^{35}$ | $1.0 \times 10^{35}$ | 9.0 |
| 12 | $0.89 \pm 0.09$ | $2.8 \pm 0.7$ | $5.5 \times 10^{-13}$ | $3.1 \times 10^{35}$ | $1.4\text{-}3.2 \times 10^{36}$ | $2.5\text{-}3.6 \times 10^{35}$ | 12.8 |
| 14 | $0.90 \pm 0.09$ | $2.4 \pm 0.7$ | $6.6 \times 10^{-13}$ | $3.6 \times 10^{35}$ | $4.5 \times 10^{35}$ | $2.4\text{-}3.6 \times 10^{35}$ | 1.9 |
| 17[b] | $1.03 \pm 0.08$ | $0.6 \pm 0.3$ | $2.1 \times 10^{-12}$ | $1.1 \times 10^{36}$ | $3.0\text{-}6.8 \times 10^{35}$ | $5.7\text{-}6.9 \times 10^{35}$ | 3.7 |
| 43 | $1.23 \pm 0.15$ | $3.2 \pm 0.9$ | $9.7 \times 10^{-13}$ | $5.8 \times 10^{35}$ | $2.3\text{-}2.9 \times 10^{35}$ | $4.0\text{-}5.8 \times 10^{35}$ | 2.5 |
| 44[b] | $1.03 \pm 0.28$ | <1.7 | $7.2 \times 10^{-13}$ | $3.8 \times 10^{35}$ | $3.6\text{-}15 \times 10^{35}$[f] | $6.5\text{-}8.6 \times 10^{35}$ | 4.2 |
| 48 | $0.97 \pm 0.48$ | <4.5 | $1.4 \times 10^{-13}$ | $7.7 \times 10^{34}$ | | $1.6\text{-}3.1 \times 10^{35}$ | 4.0 |

[a] Spectral fit to MOS spectra only; [b] spectral fit to pn spectrum only.
[c] Total column density including galactic foreground column, assuming solar element abundances.
[d] 0.2–10 keV, determined from the pn spectrum.
[e] 0.2–10 keV, intrinsic luminosity with $N_H$ set to 0, assuming a distance of 65 kpc to the SMC.
[f] The maximum luminosity was seen during a BeppoSAX observation.

Yokogawa et al. 2003). In Fig. 3 we present FFT power spectra and light curves folded at the pulse period of the four pulsars. As indicated by the presence of the first harmonic in the power spectrum of RX J0049.7−7323, the pulse profile of this long period pulsar is double peaked. The determined pulse periods with $1\sigma$ error are listed in Table 1.

From SAX J0103.2−7209 (source 44, Israel et al. 2000) which is located at the rim of the field of SNR 0103−72.6, we detect pulsations with a period of 341.2 s. This indicates that the period of large spin-up reported by (Israel et al. 2000) is now lasting more than 4.5 years (Figs. 4 and 5). In Fig. 5 we also plot period measurements of the two long period pulsars RX J0050.8−7316 and RX J0049.7−7323. The two pulsars with periods measured at more than two epochs, SAX J0103.2−7209 and RX J0050.8−7316 = AX J0051−733, show very similar pulse periods and also (linear) period changes $\dot{P}$ of $-1.6$ s yr$^{-1}$ and $-1.0$ s yr$^{-1}$, respectively. A $\dot{P}$ of $-14$ s yr$^{-1}$ is derived for the 750 s pulsar XMMU 004942.3−732313 but is based on only two period measurements, one of them with large error.

For six of the eleven sources we do not detect significant pulsations. From a $Z_1^2$ analysis no period with more than 2.5 $\sigma$ significance was found. In particular in the data of observation 0110000101 with low background, modulations with a similar pulsed fraction as seen from the detected pulsars (Fig. 3) should be easily picked up. On the other hand, the sensitivity for period detection is lower in the high-background observation 0110000301. The pulse period of SAX J0103.2−7209 was detected with a formal 3.2 $\sigma$ significance (for an unknown period) and a slightly weaker modulation would not be detected for sources 43 and 48.

### 2.3. X-ray spectra

EPIC-pn and -MOS spectra were extracted for the eleven Be/X-ray binaries and candidates and fit simultaneously. An absorbed power-law model describes the data sufficiently well (with typical reduced $\chi^2$ values around 1.0) for the given statistical quality of the spectra. Normalization factors were allowed to vary between the individual instruments to account for cross-calibration effects. Figure 6 shows an example fit to the spectra of XMMU J004942.3−732313 (source 11), the 750 s pulsar located in the field of SNR 0047−73.5. Table 2 summarizes the spectral fit results for all eleven sources. The power-law photon indices $\gamma$ show a narrow distribution with an average value of 1.0 and a standard deviation of 0.16. The total absorption column densities are above the Galactic foreground value of $5.74 \times 10^{20}$ cm$^{-2}$ as observed towards the SMC (Dickey & Lockman 1990) and indicates absorption by interstellar matter in the SMC and/or local matter around the X-ray sources. For the absorbing material solar element abundances were used in the spectral fits. If an SMC abundance of 0.2 solar is assumed (Russell & Dopita 1992), the contribution to the column density by SMC matter (total $N_H$ reduced by the Galactic foreground) needs to be multiplied by a factor of 5.0. In Table 2 we list observed fluxes and source intrinsic luminosities in the 0.2–10.0 keV energy band.

### 2.4. Long term variability

To investigate intensity variations on time scales of years we list in Table 2 the range of X-ray luminosities in which the investigated sources were detected in the past. We do this separately for instruments covering an energy band similar to the EPIC band (ASCA, BeppoSAX) and for ROSAT with the soft band of 0.1–2.4 keV. Most broad-band luminosities were reported from ASCA observations by Yokogawa et al. (2003, 0.7–10.0 keV) which were corrected by a factor of 1.05 to account for the slightly larger (0.2–10.0 keV) energy band. Only source 44 (SAX J0103.2−7209) was observed with maximum luminosity by BeppoSAX (Israel et al. 2000). In this case the correction factor is 1.23. The correction factors were

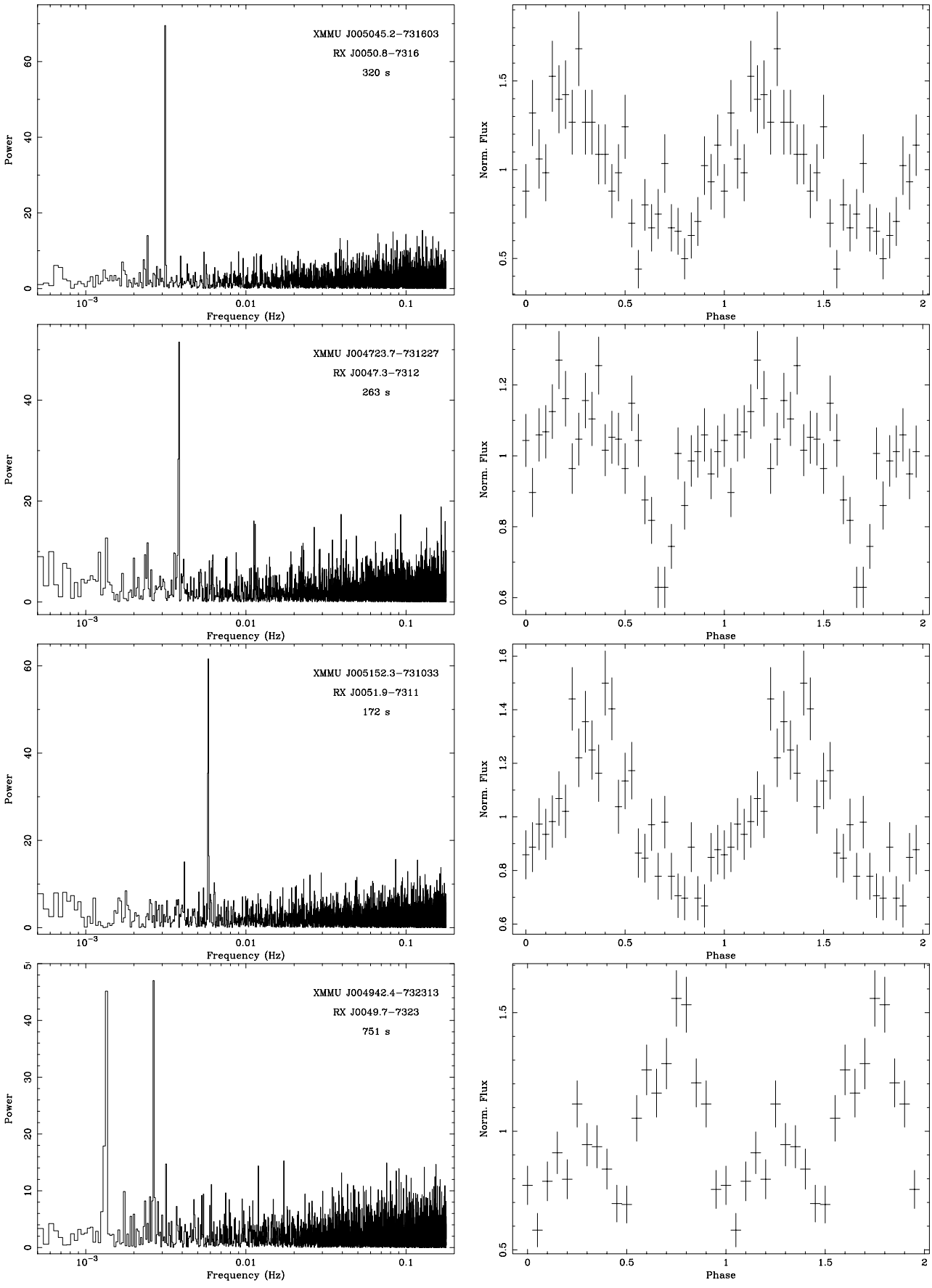


**Fig. 3.** Power spectra (left) and pulse-folded light curves (right) of X-ray pulsars in the EPIC field of SNR 0047−73.5 obtained from 0.3−7.5 keV pn data.

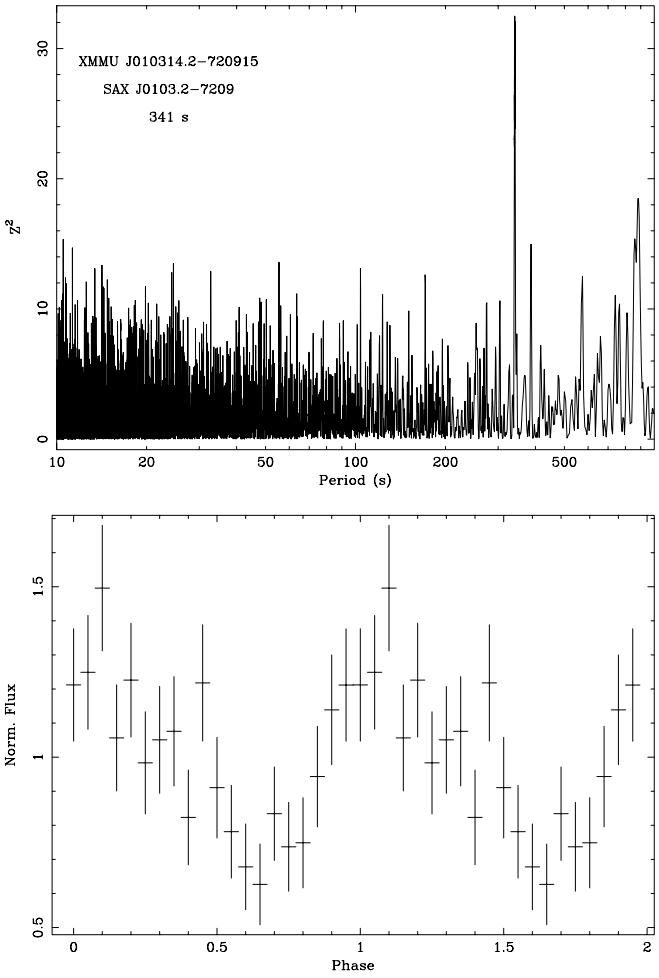


**Fig. 4.** Top: Periodogram resulting from a $Z_1^2$ test using the EPIC-pn data in the energy band 0.5−5.0 keV. Bottom: Folded pulse profile of the same data.

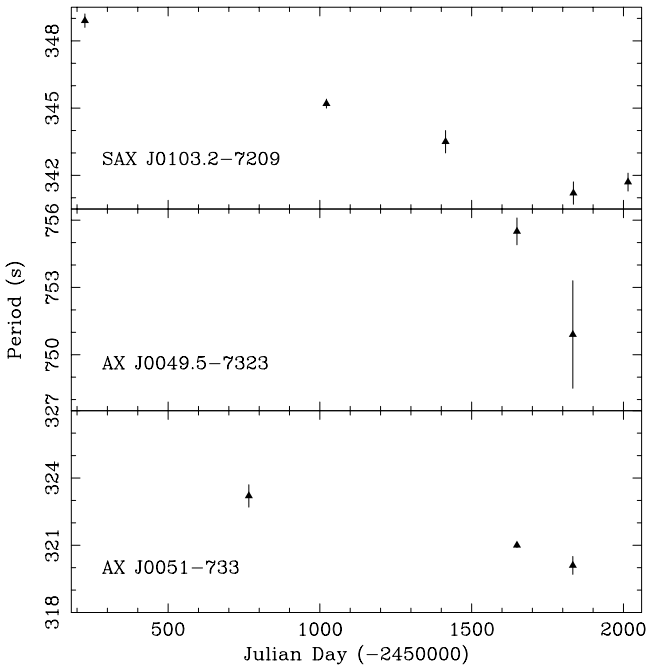


**Fig. 5.** Spin history of three long period SMC pulsars. The last data points (for SAX J0103.2−7209 the last two points with the very last taken from Sasaki et al. 2003) are XMM-Newton measurements. Previous values for the period were reported in Israel et al. (2000) and Yokogawa et al. (2003).

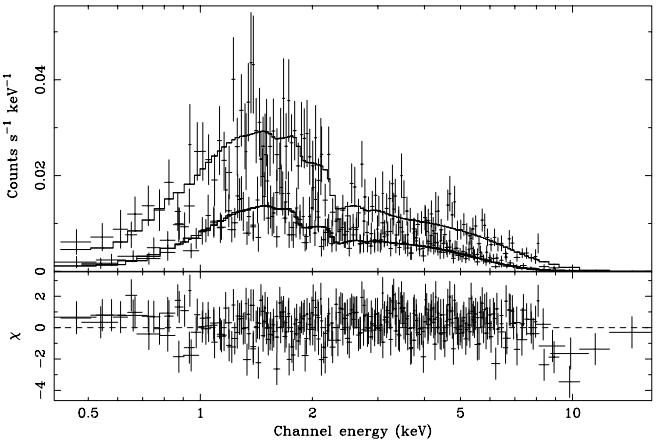


**Fig. 6.** EPIC spectra (crosses) of the pulsar RX J0049.7–7323 = AX J0049.5–7323 together with the best-fit absorbed power-law model. The model is drawn in the upper panel as histograms for the pn spectrum (upper one) and both MOS spectra (lower pair which overlaps and appears as single histogram).

derived for an unabsorbed power-law spectrum with photon index of 1.0. Source 5 was not detected by ASCA and for sources 7 and 9 the association with the nearby ASCA source 8 is unclear. We also do not give an ASCA flux for source 48 because of contamination of the spectrum by nearby sources due to the large ASCA point spread function. To obtain 0.2–10 keV luminosities based on ROSAT measurements we used the spectral parameters inferred from the EPIC spectra, computed expected PSPC count rates by folding the spectral model through the PSPC detector response and scaled the observed count rates to derive the conversion factor. Measured PSPC count rates were taken from the Results Archive (RRA) PSPC source catalogue from pointed ROSAT observations (ROSAT Consortium 2000) which contains multiple detection entries for a source if observed more than once during the ROSAT mission. The last column in Table 2 shows the ratio between maximum and minimum luminosity which is at most a factor of 13. The intensity variations are relatively moderate for this kind of object and can probably be explained by variations of the mass accretion rate along a neutron star orbit with moderate eccentricity within the circumstellar matter of the Be star. While variations up to a factor of ∼20 are observed from many Be/X-ray binaries (e.g. Haberl & Pietsch 1999), "giant" outbursts (factor 100–1000) are rare and are thought to be explained by increased mass outflow through the Be stellar wind disc (Apparao 1994). No giant outbursts were so far detected from any of the eleven systems.

## 3. The HMXB population of the SMC

The detection of a periodic 263.6 s X-ray flux modulation from XMMU J004723.7−731226 increases the number of likely HMXB pulsars in the SMC to at least thirty-seven. In Table 3 we give an updated list of HMXBs and candidates in

**Table 3.** High mass X-ray binaries and candidates in the SMC.

| 1 | 2 | 3 | 4 | 5 | 6 | 7 | 8 | 9 | 10 | 11 |
|---|---|---|---|---|---|---|---|---|---|---|
| No. | RA (J2000.0) | Dec | $r_{90}$ [″] | $S$ | HS | MA | $d_{ox}$ [″] | Period [s] | ST | Comment |
| 1 | 00 32 56.2 | −73 48 20 | 14.7 | R | 1 | | | | Be (2) | RX J0032.9−7348 (1) two Be stars |
| 2 | 00 45 37.9 | −73 13 54 | 30.2 | R | 3 | 114 | 23.4 | | Be? | RX J0045.6−7313 |
| 3[a] | 00 47 23.7 | −73 12 27 | 4.0 | N | 6 | 172 | 3.9 | 263 | Be? | RX J0047.3−7312 AX J0047.3−7312 (3) |
| 4[b] | 00 48 14.0 | −73 09 39 | 40.0 | A | | 215 | 23.3 | | Be? | AX J0048.2−7309 (3) |
| 5[a] | 00 48 34.5 | −73 02 30 | 4.1 | N | 8 | 238 | 2.2 | | Be? | RX J0048.5−7302 |
| 6 | 00 49 02.6 | −72 50 53 | 15.4 | R | 9 | | | 74.67 | Be (2,5) | RX J0049.1−7250 (1,4) AX J0049−729 (3) two Be stars |
| 7[a] | 00 49 13.8 | −73 11 37 | 4.0 | N | | | | | Be? | RX J0049.2−7311 (6) |
| 8[b] | 00 49 18.5 | −73 12 01 | 40.0 | A | | | | 9.13 | Be? | AX J0049−732 (3) |
| 9[a] | 00 49 29.9 | −73 10 58 | 4.1 | N | 10 | 300 | 1.7 | | Be? | RX J0049.5−7310 (6) |
| 10 | 00 49 33.7 | −73 31 25 | 24.2 | R | 11 | 302 | 22.2 | | Be? | RX J0049.5−7331 AX J0049.5−7330 (3) |
| 11[a] | 00 49 42.4 | −73 23 13 | 4.0 | N | 12 | 315 | 2.6 | 755.5 | Be (7) | RX J0049.7−7323 = AX J0049.5−7323 (3) |
| 12[a] | 00 50 45.2 | −73 16 03 | 4.0 | N | 13 | 387 | 3.0 | 323.2 | Be (5,8,37) | RX J0050.8−7316 = AX J0051−733 (8,3) |
| 13 | 00 50 46.9 | −73 32 48 | 34.4 | R | 14 | 393 | 9.2 | | Be? | RX J0050.7−7332 |
| 14[a] | 00 50 57.6 | −73 10 08 | 4.0 | N | 15 | 414 | 1.7 | | Be? | RX J0050.9−7310 AX J0050.8−7310 (3) |
| 15 | 00 50 56.9 | −72 13 31 | 7.1 | R | 16 | 413 | 2.7 | 91.12 | Be (2) | AX J0051−722 (9) |
| 16 | 00 51 19.6 | −72 50 44 | 17.1 | R | 17 | 447 | 14.6 | | Be? | RX J0051.3−7250 |
| 17[a] | 00 51 52.3 | −73 10 33 | 4.0 | N | 19 | 504 | 2.1 | 172 | Be (8) | RX J0051.9−7311 = AX J0051.6−7311 (8,3) |
| 18 | 00 51 53.1 | −72 31 50 | 46.3 | R | 20 | 506 | 1.1 | 8.9 | Be (2,12) | 1WGA J0051.8−7231 (1,12) |
| 19 | 00 51 54.2 | −72 55 36 | 40.0 | E | 21 | 521 | 28.3 | | Be? | (13) |
| 20 | 00 52 05.4 | −72 25 56 | 17.3 | R | 22 | 531 | 7.2 | | Be | SMC X−3 |
| 21 | 00 52 14.0 | −73 19 14 | 7.3 | R | 23 | 552 | 5.1 | 15.3 | Be (14,15) | RX J0052.1−7319 (1,14) |
| 22 | 00 52 17.0 | −72 19 51 | 111.0 | X | | 537 | 71.1 | 4.78 | Be? (19) | XTE J0052−723 (19) |
| 23 | 00 52 52.7 | −72 48 22 | 40.0 | E | 24 | 618 | 8.1 | | Be (20) | 2E0051.1−7304, AzV138 |
| 24 | 00 52 57.9 | −71 58 13 | 31.0 | R | 25 | 623 | 13.2 | 169 | Be (8) | RX J0052.9−7158 (8) XTE J0054−720 = AX J0052.9−7157 (10,3) |
| 25 | 00 53 30.0 | −72 27 28 | 27.8 | R | 26 | 667 | 31.0 | | Be? | |
| 26 | 00 53 53.4 | −72 27 01 | 26.6 | R | 27 | 717 | 22.7 | 46.63 | Be (11) | 1WGA J0053.8−7226 = XTE J0053−724 = AX J0053.9−7226 (9,3) two Be stars |
| 27 | 00 54 30.9 | −73 40 55 | 12.6 | R | 28 | | | 2.37 | Be | SMC X−2 (38,3) |
| 28 | 00 54 33.2 | −72 28 09 | 46.2 | R | 29 | 772 | 26.6 | | Be? | |
| 29 | 00 54 55.4 | −72 45 06 | 9.0 | R | 30 | 809 | 4.7 | | Be? | AX J0054.8−7244 (3) |
| 30 | 00 54 56.0 | −72 26 49 | 4.1 | N | 31 | 810 | 1.6 | 59.07 | Be (2,5) | XTE J0055−724 = 1SAX J0054.9−7226 = 1WGA J0054.9−7226 (21,22,23) |
| 31 | 00 56 05.2 | −72 22 01 | 4.5 | N | 32 | 904 | 3.2 | 140.1 | Be? | XMMU J005605.2−722200 2E0054.4−7237 (23) |
| 32 | 00 57 26.8 | −73 25 02 | 21.1 | R | | | | 101 | Be? | RX J0057.4−7325 AX J0057.4−7325 (3) (7) |
| 33 | 00 57 36.3 | −72 19 35 | 1.1 | C | | 1020 | 1.6 | 565 | Be? | CXOU J005736.2−721934 (23,24) |
| 34 | 00 57 50.2 | −72 02 37 | 4.1 | N | 35 | 1036 | 3.5 | 280.4 | Be? | RX J0057.8−7202 = AX J0058−72.0 (3,23) |
| 35 | 00 57 50.3 | −72 07 57 | 1.0 | C | 36 | 1038 | 0.7 | 152.3 | Be? | CXOU J005750.3−720756 (23,24) |
| 36 | 00 57 59.5 | −71 56 37 | 20.4 | R | 37 | 1044 | 21.1 | | Be? | |
| 37 | 00 58 11.7 | −72 30 50 | 4.3 | N | 38 | | | | Be (7,8) | RX J0058.2−7231 (8,23) |
| 38 | 00 59 11.4 | −71 38 45 | 7.5 | R | 40 | –179 | 10.1 | 2.763 | Be (26) | RX J0059.2−7138 (25) |
| 39 | 01 00 30.2 | −72 20 35 | 5.1 | N | | 1208 | 2.1 | | Be? | XMMU J010030.2−722035 (23) |
| 40 | 01 01 02.8 | −72 06 58 | 1.2 | C | 42 | 1240 | 1.1 | 304.5 | Be (2,7) | RX J0101.0−7206 (1,24) |
| 41 | 01 01 20.8 | −72 11 21 | 4.1 | N | 43 | 1257 | 2.1 | 455 | Be (27) | RX J0101.3−7211 (27) |
| 42 | 01 01 37.6 | −72 04 19 | 4.1 | N | 44 | 1277 | 5.2 | | Be? | RX J0101.6−7204 (23) |
| 43[a] | 01 01 52.4 | −72 23 36 | 4.1 | N | 45 | 1288 | 2.8 | | Be? | AX J0101.8−7223 (3) XMMU J010152.4−722336 |
| 44[a] | 01 03 14.2 | −72 09 15 | 4.1 | N | 49 | 1367 | 1.1 | 345.2 | Be (29,5) | SAX J0103.2−7209 = AX J0103.2−7209 = CXOU J010314.1−720915 (28) |
| 45 | 01 03 37.6 | −72 01 33 | 4.0 | N | 50 | 1393 | 1.1 | | Be? | RX J0103.6−7201 (23) |
| 46 | 01 04 07.4 | −72 43 59 | 19.0 | R | 51 | 1440 | 9.0 | | Be? | or AGN? 13 cm |
| 47[b] | 01 04 35.7 | −72 21 43 | 7.4 | R | 52 | 1470 | 4.0 | | Be? | RX J0104.5−7221 |
| 48[a] | 01 05 09.8 | −72 11 46 | 4.2 | N | 53 | | | 3.34? | Be? | RX J0105.1−7211 AX J0105−722 (3,30) |

**Table 3.** continued.

| No. | RA (J2000.0) | Dec | $r_{90}$ [″] | $S$ | HS | MA | $d_{ox}$ [″] | Period [s] | ST | Comment |
|---|---|---|---|---|---|---|---|---|---|---|
| 49 | 01 05 55.4 | −72 03 48 | 4.3 | N | 55 | 1557 | 3.2 | | Be? | RX J0105.9−7203 AX J0105.8−7203 (3,23) |
| 50 | 01 07 10.9 | −72 35 37 | 13.1 | R | 56 | 1619 | 10.1 | | Be? | AX J0107.2−7234 (3) |
| 51 | 01 11 14.5 | −73 16 50 | 61.2 | R | 58 | 1747 | 63.9 | 31.03 | Be (15,16) | XTE J0111.2−7317 = AX J0111.1−7316 (17,18,3) |
| 52 | 01 17 05.5 | −73 26 33 | 7.0 | R | | | | 0.717 | SG | SMC X−1 |
| 53 | 01 17 41.5 | −73 30 50 | 7.0 | R | 59 | 1845 | 4.3 | 22.07 | Be (32) | RX J0117.6−7330 (31) |
| 54 | 01 19 37.7 | −73 30 06 | 14.7 | R | 60 | 1867 | 8.3 | | Be? | |
| 55 | | | | X | | | | 2.165 | | XTE J0119-731 (40) |
| 56 | | | | X | | | | 6.85 | | XTE J0103-728 (39) |
| 57 | | | | X | | | | 7.8 | | (36) |
| 58 | | | | X | | | | 16.6 | | XTE J0050−732#1 (35) ≠ RX J0051.9−7311 |
| 59 | | | | X | | | | 25.5 | | XTE J0050−732#2 (35) |
| 60 | | | | X | | | | 46.4 | | XTE pulsar (33) |
| 61 | | | | X | | | | 82.4 | | XTE J0052−725 (33) |
| 62 | | | | X | | | | 89 | | (39) |
| 63 | | | | X | | | | 95 | | XTE SMC95 (34) |
| 64 | | | | X | | | | 144.1 | | XTE SMC144s (39) |
| 65 | | | | X | | | | 164.7 | | (39) |

[a] Source investigated in this work. [b] Source not detected by XMM-Newton in this work.
For sources 55-65 no X-ray positions are listed due to their large uncertainties and we list them sorted by pulse period.
Notes to specific columns: (2, 3, 4) Best available X-ray position with error. For ROSAT and XMM-Newton positions systematic uncertainties of 7″ and 4″ are included. (5) X-ray mission which provided the data for the best position (A: ASCA, C: Chandra, E: Einstein, N: XMM-Newton, R: ROSAT, X: RXTE). (6) as Table 1. (7) Nearest H$\alpha$ emission line object consistent with the X-ray position from the catalogues of Meyssonnier & Azzopardi (1993) and Murphy & Bessell (2000, in the case of source 38 which is indicated by a negative entry number). (8) as Table 1. (10) HMXB sub-type, Be or supergiant (SG); Be? indicates an H$\alpha$ emission line object as possible counterpart, no optical spectrum is available in the literature in this case. (11) Likely cross identifications of X-ray sources detected with different missions (a "=" between source names indicates a secure identification based on positional coincidence and detection of pulsations, the ≠ in the comment to source 58 marks that the ROSAT source is not the counterpart of the RXTE source, see also source 17).
References given in parenthesis in columns 10 and 11:
(1) Kahabka & Pietsch (1996), (2) Stevens et al. (1999), (3) Yokogawa et al. (2003), (4) Kahabka & Pietsch (1998), (5) Coe & Orosz (2000), (6) Filipović et al. (2000b), (7) Edge & Coe (2003), (8) Schmidtke et al. (1999), (9) Corbet et al. (1998), (10) Lochner et al. (1998), (11) Buckley et al. (2001), (12) Israel et al. (1997), (13) Wang & Wu (1992), (14) Finger et al. (2001), (15) Covino et al. (2001), (16) Coe et al. (2000), (17) Chakrabarty et al. (1998), (18) Wilson & Finger (1998), (19) Laycock et al. (2003), (20) Garmany & Humphreys (1985), (21) Marshall & Lochner (1998), (22) Santangelo et al. (1998), (23) Sasaki et al. (2003), (24) Macomb et al. (2003), (25) Hughes (1994), (26) Southwell & Charles (1996), (27) Sasaki et al. (2001), (28) Israel et al. (2000), (29) Hughes & Smith (1994), (30) Filipović et al. (2000a), (31) Macomb et al. (1999), (32) Clark et al. (1997), (33) Corbet et al. (2002), (34) Laycock et al. (2002), (35) Lamb et al. (2002b), (36) Corbet et al. (2003b), (37) Coe et al. (2002), (38) Corbet et al. (2001), (39) Corbet et al. (2003c), (40) Corbet et al. (2003a).

the SMC which is based on the work of HS00 and add transient pulsars detected by RXTE. We do not include two additional known pulsars which may be of different type: AX J0043−737 for which confirmation of a 87 ms period is needed and which could be a Crab-like pulsar (Yokogawa & Koyama 2000; Yokogawa et al. 2003), and CXOU J0110043.1−721134 a possible anomalous X-ray pulsar in the SMC (Lamb et al. 2002a).

The number of Be/X-ray binaries and candidates is the highest known for any galaxy, including the Milky Way where about forty such systems (Liu et al. 2000) are known today. The SMC Be/X-ray binaries, all at a similar distance, constitute an ideal sample for statistical studies. Luminosity distributions were derived by HS00 and Sasaki et al. (2003). Compared to the Milky Way the SMC harbours a higher fraction of low-luminosity systems ($\sim 10^{35}$ erg s$^{-1}$), which may be a selection effect due to a more difficult identification of such objects in the Galactic Plane (HS00). The XMM-Newton results from SMC HMXBs make it possible to compare the X-ray spectra from already 16 sources (11 from this work and sources 33, 34, 35, 41 and 45 from Sasaki et al. 2003) obtained with the same instruments and processed in a coherent way. In Fig. 7 (upper panel) the distribution of the power-law photon index is presented. The distribution is strongly peaked at 1.0, but includes a weak wide contribution with indices between 0.65 and 1.45.

Although the column densities derived from the spectra have relatively large errors, the $N_{\rm H}$ distribution (Fig. 7 bottom panel) exhibits two maxima. An excess of objects with little or no absorption may either indicate spectra with a soft component which is not recognized because of insufficient statistics or a special spatial distribution of the sources on the near side of the SMC (star-formation arm). The second peak may be explained by interstellar absorption in the SMC with the majority

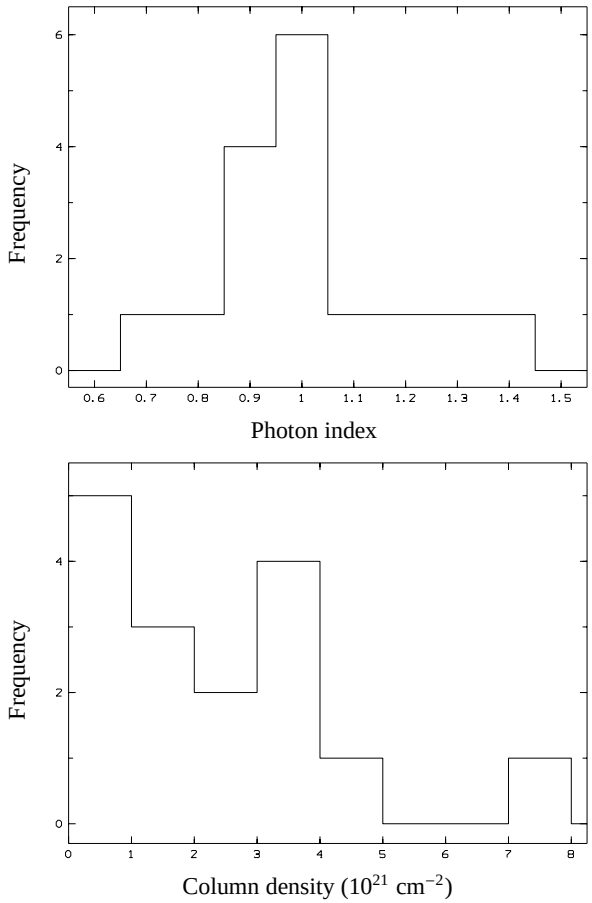


**Fig. 7.** Distribution of power-law photon indices (top) and absorption column density (bottom, without Galactic absorption) measured from EPIC spectra of sixteen Be/X-ray binaries and candidates in the SMC observed by the EPIC instruments of XMM-Newton.

of objects located in the inner parts of the SMC. A comparison with similar data obtained from background AGN behind the SMC should make it possible to derive constraints on the total absorbing column density through the SMC on a statistical basis.

## 4. Summary

We performed temporal and spectral analysis of eleven Be/X-ray binaries and candidates observed serendipitously by the EPIC instruments on board XMM-Newton in two observations of the supernova remnants SNR 0047−73.5 and SNR 0103−72.6. From five of the objects pulsations in their X-ray flux are detected, four of them were previously known pulsars and in one case, XMMU J004723.7−731227, the XMM-Newton data revealed 263 s pulsations for the first time. XMMU J004723.7−731227 coincides in position with RX J0047.3−7312 which was suggested to be a Be/X-ray binary due to its likely identification with an H$\alpha$ emission line object (HS00). The detection of the pulse period strongly supports this identification.

The detection of pulsations, together with the good X-ray positions allowed to securely identify sources detected by various X-ray space missions, like e.g. the 172 s pulsar AX J0051.6−7311 with XMMU J005152.2−731033 (via pulsations) and RX J0051.9−7311 (via accurate position). The latter was previously also suggested to be the counterpart of XTE J0050−732#1, a 16.6 s pulsar. The 345 s pulsar SAX J0103.2−7209 was found to continue its large spin down with a rate of $-1.6$ s yr$^{-1}$ extending now over 4.5 years. The 323 s pulsar AX J0051−733 was found to exhibit very similar properties as SAX J0103.2−7209 with respect to spin period, period derivative and X-ray luminosity.

The large number of Be/X-ray binaries in the SMC allows first statistical studies of their spectral and temporal properties. XMM-Newton and Chandra are ideally suited to detect pulsars among the Be-/X-ray binary candidates at low source fluxes and future observations are required to further increase the sample and allow to analyse it in a homogeneous way.

*Acknowledgements.* The XMM-Newton project is supported by the Bundesministerium für Bildung und Forschung/Deutsches Zentrum für Luft- und Raumfahrt (BMBF/DLR), the Max-Planck-Gesellschaft and the Heidenhain-Stiftung.

## References

Apparao, K. M. V. 1994, Space Sci. Rev., 69, 255
Barcons, X., Carrera, F. J., Watson, M. G., et al. 2002, A&A, 382, 522
Buckley, D. A. H., Coe, M. J., Stevens, J. B., et al. 2001, MNRAS, 320, 281
Chakrabarty, D., Levine, A. M., Clark, G. W., & Takeshima, T. 1998, IAU Circ., 7048, 1
Clark, G. W., Remillard, R. A., & Woo, J. W. 1997, ApJ, 474, L111
Coe, M. J., Haigh, N. J., Laycock, S. G. T., Negueruela, I., & Kaiser, C. R. 2002, MNRAS, 332, 473
Coe, M. J., Haigh, N. J., & Reig, P. 2000, MNRAS, 314, 290
Coe, M. J., & Orosz, J. A. 2000, MNRAS, 311, 169
Corbet, R., Marshall, F. E., Lochner, J. C., Ozaki, M., & Ueda, Y. 1998, IAU Circ., 6803, 1
Corbet, R. H. D., Marshall, F. E., Coe, M. J., Laycock, S., & Handler, G. 2001, ApJ, 548, L41
Corbet, R., Markwardt, C. B., Marshall, F. E., Laycock, S., & Coe, M. 2002, IAU Circ., 7932, 2
Corbet, R., Markwardt, C. B., Marshall, F. E., et al. 2003a, IAU Circ., 8064, 4
Corbet, R. H. D., Edge, W. R. T., Laycock, S., et al. 2003b, AAS/High Energy Astrophysics Division, 35, 1
Corbet, R. H. D., Markwardt, C. B., Marshall, F. E., et al. 2003c, The Astronomer's Telegram, 163, 1
Covino, S., Negueruela, I., Campana, S., et al. 2001, A&A, 374, 1009
Dickey, J. M., & Lockman, F. J. 1990, ARA&A, 28, 215
Edge, W. R. T., & Coe, M. J. 2003, MNRAS, 338, 428
Filipović, M. D., Haberl, F., Pietsch, W., & Morgan, D. H. 2000a, A&A, 353, 129
Filipović, M. D., Pietsch, W., & Haberl, F. 2000b, A&A, 361, 823
Finger, M. H., Macomb, D. J., Lamb, R. C., et al. 2001, ApJ, 560, 378
Garmany, C. D., & Humphreys, R. M. 1985, AJ, 90, 2009
Haberl, F., Filipović, M. D., Pietsch, W., & Kahabka, P. 2000, A&AS, 142, 41
Haberl, F., & Pietsch, W. 1999, A&A, 344, 521
Haberl, F., & Sasaki, M. 2000, A&A, 359, 573

Hughes, J. P. 1994, ApJ, 427, L25
Hughes, J. P., & Smith, R. C. 1994, AJ, 107, 1363
Israel, G. L., Campana, S., Covino, S., et al. 2000, ApJ, 531, L131
Israel, G. L., Stella, L., Angelini, L., et al. 1997, ApJ, 484, L141
Kahabka, P., & Pietsch, W. 1996, A&A, 312, 919
Kahabka, P., & Pietsch, W. 1998, IAU Circ., 6840, 1
Lamb, R. C., Fox, D. W., Macomb, D. J., & Prince, T. A. 2002a, ApJ, 574, L29
Lamb, R. C., Macomb, D. J., Prince, T. A., & Majid, W. A. 2002b, ApJ, 567, L129
Laycock, S., Corbet, R. H. D., Coe, M. J., et al. 2003, MNRAS, 339, 435
Laycock, S., Corbet, R. H. D., Perrodin, D., et al. 2002, A&A, 385, 464
Liu, Q. Z., van Paradijs, J., & van den Heuvel, E. P. J. 2000, A&AS, 147, 25
Lochner, J. C., Marshall, F. E., Whitlock, L. A., & Brandt, N. 1998, IAU Circ., 6814, 1
Macomb, D. J., Finger, M. H., Harmon, B. A., Lamb, R. C., & Prince, T. A. 1999, ApJ, 518, L99
Macomb, D. J., Fox, D. W., Lamb, R. C., & Prince, T. A. 2003, ApJ, 584, L79
Marshall, F. E., & Lochner, J. C. 1998, IAU Circ., 6818, 1
Mereghetti, S. 2001, in Frontier Objects in Astrophysics and Particle Physics, Vulcano Workshop, 21–27 May, 2000, ed. F. Giovannelli, & G. Mannocchi (Italian Physical Society), 239
Meyssonnier, N., & Azzopardi, M. 1993, A&AS, 102, 451
Murphy, M. T., & Bessell, M. S. 2000, MNRAS, 311, 741
ROSAT Consortium 2000, ROSAT News, 72, 1
Russell, S. C., & Dopita, M. A. 1992, ApJ, 384, 508
Santangelo, A., Cusumano, G., Israel, G. L., et al. 1998, IAU Circ., 6818, 1
Sasaki, M., Haberl, F., Keller, S., & Pietsch, W. 2001, A&A, 369, L29
Sasaki, M., Haberl, F., & Pietsch, W. 2000, A&AS, 147, 75
Sasaki, M., Pietsch, W., & Haberl, F. 2003, A&A, 403, 901
Schmidtke, P. C., Cowley, A. P., Crane, J. D., et al. 1999, AJ, 117, 927
Southwell, K. A., & Charles, P. A. 1996, MNRAS, 281, L63
Stevens, J. B., Coe, M. J., & Buckley, D. A. H. 1999, MNRAS, 309, 421
Strüder, L., Briel, U., Dennerl, K., et al. 2001, A&A, 365, L18
Turner, M. J. L., Abbey, A., Arnaud, M., et al. 2001, A&A, 365, L27
Wang, Q., & Wu, X. 1992, ApJS, 78, 391
Wilson, C. A., & Finger, M. H. 1998, IAU Circ., 7048, 2
Yokogawa, J., Imanishi, K., Tsujimoto, M., Koyama, K., & Nishiuchi, M. 2003, PASJ, 55, 161
Yokogawa, J., & Koyama, K. 2000, IAU Circ., 7361, 2